

Non-collinear long-range magnetic ordering in HgCr_2S_4

L.C. Chapon,¹ P.G. Radaelli,^{1,2} Y. S. Hor,³ M.T.F. Telling,¹ and J.F. Mitchell³

¹*ISIS facility, Rutherford Appleton Laboratory-CCLRC,
Chilton, Didcot, Oxfordshire, OX11 0QX, United Kingdom.*

²*Dept. of Physics and Astronomy, University College London,
Gower Street, London WC1E 6BT, United Kingdom*

³*Materials Science Division, Argonne National Laboratory, Argonne, IL 60439*

The low-temperature magnetic structure of HgCr_2S_4 has been studied by high-resolution powder neutron diffraction. Long-range incommensurate magnetic order sets in at $T_N \sim 22\text{K}$ with propagation vector $\mathbf{k}=(0,0,\sim 0.18)$. On cooling below T_N , the propagation vector increases and saturates at the commensurate value $\mathbf{k}=(0,0,0.25)$. The magnetic structure below T_N consists of ferromagnetic layers in the ab -plane stacked in a spiral arrangement along the c -axis. Symmetry analysis using corepresentations of the little group reveals a crystal point symmetry 432 (O), which is incompatible with macroscopic ferroelectricity. This finding indicates that the spontaneous electric polarization observed experimentally cannot be coupled to the magnetic order parameter.

PACS numbers: 25.40.Dn, 75.25.+z, 77.80.-e

There has been a considerable renewal of interest in multiferroic materials in the last few years, in particular in magnetoelectric oxides such as TbMnO_3 ¹, TbMn_2O_5 ^{2,3} or the Kagomé staircase compound $\text{Ni}_3\text{V}_2\text{O}_8$ ⁴. These systems commonly exhibit strong magnetic frustration due to the presence of competing interactions or geometrical constraints. Additionally, their magnetically ordered states are typically quite complex, and they are all improper ferroelectrics. Independent of the microscopic mechanism responsible for ferroelectricity-antisymmetric Dzyalozinski-Moriya interaction or symmetric exchange striction-the symmetry breaking process associated with long-range magnetic order leaves a non-centrosymmetric structural point group, allowing a macroscopic spontaneous polarization to develop below the magnetic critical temperature. Another common behavior of fundamental interest in these systems, is the nature of magnetic ordering itself, which involve propagation vector systematically inside the Brillouin zone, whether magnetic order is commensurate or not with respect to the crystalline unit cell. In these cases, it is crucial to perform symmetry analysis using co-representation theory to capture the full structural point group symmetry⁵.

Recently, attention has been drawn to chalcogenide chromium spinels of the type ACr_2X_4 ($\text{A}=\text{Cd},\text{Hg}$; $\text{X}=\text{S},\text{Se}$) which are weakly ferroelectric in their magnetically ordered state and have been classified as multiferroic materials^{6,7,8}. However, the dielectric behaviors are reminiscent of relaxor ferroelectrics, in which polar domains of nanometric sizes appear below the critical temperature. Although most chalcogenide spinels are Heisenberg ferromagnets, HgCr_2S_4 shows a more complex magnetic behavior at low temperature, indicating stronger competition between short- and long-range interactions: despite a large positive Weiss temperature of 142K ⁹, indicating dominant ferromagnetic interactions, the low temperature magnetic structure found by neutron diffraction experiments¹⁰ corresponds to a non

collinear antiferromagnet, in agreement with recent bulk magnetization measurements⁸. However, Weber and co-workers noted in⁷ that *the true nature of the magnetic state of HgCr_2S_4 still needs some clarification* due to discrepancies between recent magnetization results⁸ and the earlier neutron¹⁰ and optical studies¹¹. Specifically, these earlier reports claim a much higher transition temperature than that of Weber et al. Also, determination of the exact magnetic ground state, including its symmetry properties, is of crucial importance to study the potential coupling of magnetic and ferroelectric order parameters and motivated the present work.

In this Communication, we report a complete analysis of the magnetic structure of HgCr_2S_4 studied by high-resolution neutron powder diffraction. Our results unambiguously demonstrate that $T_N \sim 22\text{K}$, in agreement with recent magnetization and specific heat measurements⁸ and contradicting early neutron diffraction and optical studies^{10,11} that reported a transition temperature around 60 K. The magnetic structure is incommensurate at T_N , but the propagation vector rapidly evolves with decreasing temperature, becoming commensurate at 1.5 K. We also report the symmetry properties of the low-temperature magnetic structure as analyzed using corepresentation theory¹². We find that only a single mode belonging to a two-dimensional irreducible co-representation of the little group fits the experimental data at 1.5 K. The resulting ordered magnetic structure refined from the neutron data is a spiral with propagation vector parallel to its axis. Symmetry analysis reveals that the structural point group associated with this magnetic configuration is 432, forbidding the development of a macroscopic polar vector. This result clearly leads to the conclusion that the appearance of hysteresis loops in the electric spontaneous polarization below 70K ⁷ $\gg T_N$ are likely related to the onset of short-range ferromagnetic correlations appearing around the same temperature.

Polycrystalline HgCr_2S_4 was synthesized by com-

binning powders of Cr (99.99%) and S (99.999%) with liquid Hg (99.9998%) mixed in a stoichiometric ratio. The mixture was sealed in an evacuated quartz tube and heated slowly to 600 °C for several days. The powder was then ground, pelletized, and sealed again for sintering at 800 °C for several weeks. Powder neutron diffraction data were collected on the high-resolution OSIRIS diffractometer at the ISIS pulsed neutron source (UK). A 1.5g sample was enclosed in a vanadium can placed in a helium cryostat. Long scans were recorded above (30K) and below (1.5K) T_N to solve the magnetic structure. Shorter scans in a narrower d-spacing range (5.2-6.4Å) were recorded between 1.5K and 25.5K in 1K steps to follow the temperature dependence of the (111)+ \mathbf{k} Bragg peak. Rietveld refinements were performed with the program FullProf¹³. Symmetry analysis using representation theory has been performed with the software MODY¹⁴. Co-representations are presented in Kovalev's convention¹².

Atoms	Cr ₁	Cr ₂	Cr ₃	Cr ₄
$\Gamma_5(1-1)$	$\epsilon^{2*}(1,i,0)$	(1,i,0)	$\epsilon^*(1,i,0)$	$\epsilon^{3*}(1,i,0)$
$\Gamma_5(1-2)$	$\epsilon^{2*}(1,-i,0)$	(1,-i,0)	$\epsilon^*(1,-i,0)$	$\epsilon^{3*}(1,-i,0)$
$\Gamma_5(2-1)$	$\epsilon^{2*}(-i,1,0)$	(-i,1,0)	$\epsilon^*(i,-1,0)$	$\epsilon^{3*}(i,-1,0)$
$\Gamma_5(2-2)$	$\epsilon^{2*}(i,1,0)$	(i,1,0)	$\epsilon^*(-i,-1,0)$	$\epsilon^{3*}(-i,-1,0)$

TABLE I: Symmetrized in-plane basis vectors for the co-representations Γ_5 . $\epsilon = e^{-i\frac{\pi}{2}\delta}$, and ϵ^* is the complex conjugate of ϵ . The atomic positions of Cr_{*i*} (*i*=1,4) are given in the text.

The neutron powder diffraction pattern collected at 30 K is consistent with the cubic crystal structure¹⁵, space group $Fd\bar{3}m$ ¹⁸. The high neutron absorption cross-section of Hg and reduced Q-range intrinsic to this instrument prevent us from extracting reliable thermal parameters and from probing possible off-center displacement of the Cr atoms recently suggested⁸. A detailed temperature-dependent structural investigation by X-ray diffraction is currently underway and will be reported elsewhere. At 1.5K, 12 magnetic Bragg peaks appear at low-Q in the diffraction pattern; all can be indexed with the propagation vector $\mathbf{k}=(0,0,\delta)$ (with respect to the F-centered cell) in agreement with a previous study¹⁰. $\delta \sim \frac{1}{4}$ within our experimental resolution, i.e. the periodicity of the magnetic structure is commensurate with respect to the nuclear unit-cell at 1.5 K.

The symmetry-allowed magnetic structures have been determined by co-representation analysis. Here we consider four Cr atoms in the primitive unit-cell (labelled Cr_{*i*} *i*=1,4) respectively positioned at $(\frac{1}{2}, \frac{1}{2}, \frac{1}{2})$, $(\frac{1}{4}, \frac{3}{4}, 0)$, $(\frac{3}{4}, 0, \frac{1}{4})$, $(0, \frac{1}{4}, \frac{3}{4})$. The remaining 12 atoms are generated by F-centering operations. The magnetic representation Γ of dimension 12 is reduced into the direct sum of irreducible representations:

$$\Gamma = \Gamma_1^1 + 2\Gamma_2^1 + 2\Gamma_3^1 + \Gamma_4^1 + 3\Gamma_5^2 \quad (1)$$

where the subscripts label the irreducible representations following Kovalev's notation¹² and the superscripts refer to their dimensionality. The magnetic transition is continuous, and according to the Landau theory of phase transitions¹⁶, should involve a single irreducible representation. Indeed, the magnetic structure is found to be consistent only with Γ_5 , with modes in the *ab*-plane. The symmetrized in-plane basis vectors for the co-representation Γ_5 are reported in Table I. Only the modes labelled $\Gamma_5(1-1)$ and $\Gamma_5(1-2)$ fit the data. Both of these modes correspond to spiral arrangements that only differ by their rotation direction, as seen from the sign of the imaginary part of the Fourier coefficients. The phases for atoms 1-4 are fixed by symmetry and are directly related to the fractional position along *c* in such a way that atoms belonging to a same plane (including atoms generated by F-centering translations) have the same phase. The magnetic structure is therefore modeled by a single parameter: the magnitude of the Fourier component, i.e. magnetic moment.

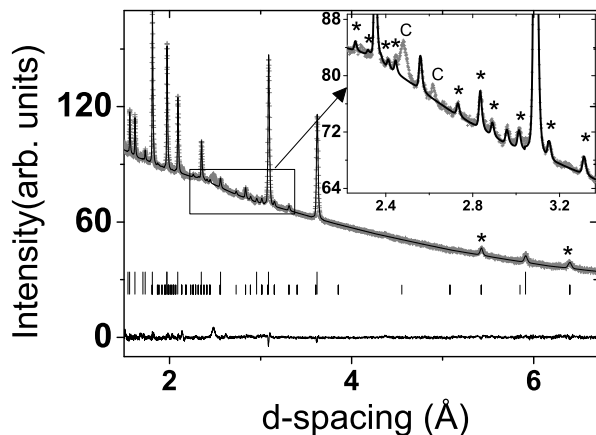


FIG. 1: Rietveld refinement of the neutron diffraction pattern for HgCr₂S₄ at 1.5K. The grey crosses represent the experimental data while the black solid line represents the refined model. The solid line at the bottom is the difference curve between data and refinement. The long (short) tick-marks show the positions of nuclear (magnetic) Bragg reflections. Non-extinct magnetic reflections are marked by an asterisk symbol. Two un-indexed diffraction peak, marked by "C", correspond to parasitic scattering from the cryostat.

The refinement of the neutron diffraction pattern at 1.5K is presented in Fig. 1, showing essentially perfect agreement between experimental data and model. As mentioned before, the magnetic structure shown in Fig. 2 corresponds to a simple spiral propagating along *c* and ferromagnetic arrangements in the *ab*-plane. Within a tetrahedral Cr₄ unit of the pyrochlore lattice, the angle between first neighbors spins along *c* is $\alpha = \pi\delta/2$, i.e. 22.5 ° at 1.5K. The magnetic moment of 2.7(1) μ_B is slightly smaller than the expected spin-only contribution

for Cr^{3+} , $S=3/2$. This value agrees well with previous studies¹⁰ and seems to indicate that a small fraction of the magnetic moment remain disordered at low temperature. Nevertheless, one must take this result with care due to the strong correlation between magnitude of the moment and absorption correction in the refinement.

On warming, the propagation vector deviates from $\delta = \frac{1}{4}$ at 4K and its magnitude decreases rapidly at higher temperature (Fig. 3) which corresponds to a monotonous variation of the angle α . It is difficult to ascribe the low temperature result where $\delta = \frac{1}{4}$ to a lock-in transition, due to the narrow temperature region in which this behavior occurs. Nonetheless, there is a clear tendency towards saturation at this value. The variation of the intensity of the $(111)+\mathbf{k}$ magnetic reflection, presented in Fig. 3., indicates a Néel transition around 22.5K, in excellent agreement with recent specific heat results showing a lambda anomaly at 22K⁸ and the strong decrease of the magnetization at low magnetic field. However, this finding contradicts earlier neutron and optical studies^{10,11} suggesting the long range ordered magnetic state persists up to 60K. Also in contradiction with¹⁰, the magnetic order parameter obeys a power law close to T_N .

When considering the origin of the magnetic structure of HgCr_2S_4 one can eliminate direct exchange at first approximation because of the larger interatomic Cr-Cr distance than those found in analogous oxide spinels. The very nature of the magnetic structure therefore indicates that antiferromagnetic next nearest neighbor interactions compete directly with ferromagnetic super-exchange Cr-S-Cr interactions. The parameter that seems to control the nature of the magnetic ground state is the Cr-S-Cr angle. In HgCr_2S_4 this angle is 98° at room temperature according to structural parameters derived by⁸, larger than for ferromagnetic CdCr_2S_4 , for which the value is 96.9° ¹⁵. This is in agreement with superexchange theory since larger deviation from 90° angles, for which antiferromagnetic correlation due to electron transfer is forbidden by symmetry, will increase the orbital overlap. The apparent extreme sensitivity of magnetic structure to angle in these compounds calls for a systematic study of the magnetic properties as a function of the averaged Cr-S-Cr bond angle.

Next we consider the ferroelectricity of HgCr_2S_4 ⁷ and demonstrate it cannot arise from coupling to the magnetic order parameter. The onset of ferroelectricity induced by symmetry breaking associated with the long-range magnetic order can be directly determined by symmetry analysis of the magnetic structure. In cases where \mathbf{k} lies inside the Brillouin zone (\mathbf{k} and $-\mathbf{k}$ are not related by a reciprocal lattice vector), only the use of co-representation theory can capture the full symmetry properties. In Table II, we report the matrix representatives of the symmetry operations of the little group $G_{\mathbf{k}}$ for the irreducible corepresentations Γ_5 . All matrices for the proper operations, or proper operations combined with the complex conjugation operator K , are diagonal.

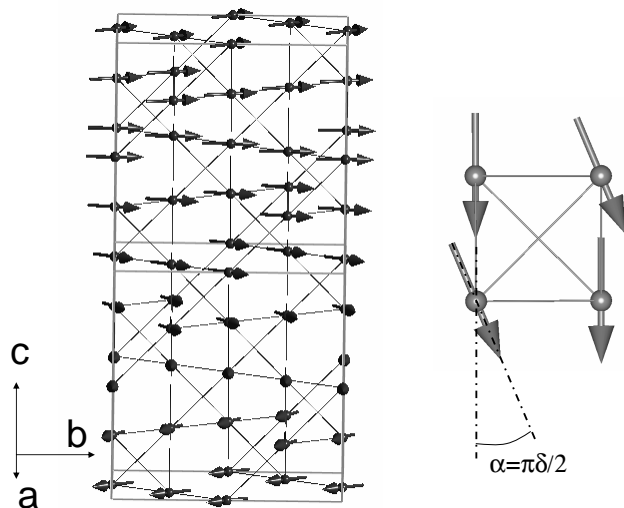


FIG. 2: Left: Magnetic structure at 1.5K showing a spiral arrangement of ferromagnetic layers in the ab -plane. Only Cr atoms/spins are shown as grey spheres/arrows. Cr atoms are connected by thin grey lines showing the underlying pyrochlore lattice. Two unit-cells along the c -direction are represented. Right: Spin-configuration within an isolated tetrahedral Cr_4 unit.

In other words, these operations transform a basis function of the two-dimensional subspace into itself, modulo a phase factor (which is equivalent to a translation for incommensurate \mathbf{k} -vectors), and are therefore symmetry operators of the structural point group. On the contrary, the matrices for improper operations are off-diagonal, which means that these operators are not preserved in the magnetically ordered state. From the list of symmetry operators preserved, one can deduce the structural point group 432 (O in Schoenflies notation). Notably, this point group is *inconsistent* with the development of a macroscopic polar vector.

The condition for ferroelectric order in non-collinear magnets has also been recently discussed phenomenologically by M. Mostovoy¹⁷. Mostovoy has shown that magnetically induced ferroelectric order can develop in non-collinear magnets only if the vector product between the spin rotation axis \mathbf{e} of the magnetic structure and propagation vector \mathbf{k} is nonzero, a condition obviously not fulfilled here since \mathbf{k} and \mathbf{e} are collinear.

The origin of ferroelectricity and associated phenomenal magnetoelectric properties in HgCr_2S_4 remains an open question. We have demonstrated conclusively that, symmetry breaking of the magnetic structure does not support a ferroelectric state. However, the hysteresis loops of the electric polarization appear below $\sim 70\text{K}$. It is possible that the ferroelectric state could be coupled to short-range ferromagnetic correlations developing around the same temperature. The presence of nanopolar regions is in agreement with this picture. However in this scenario, one might expect an abrupt decrease of

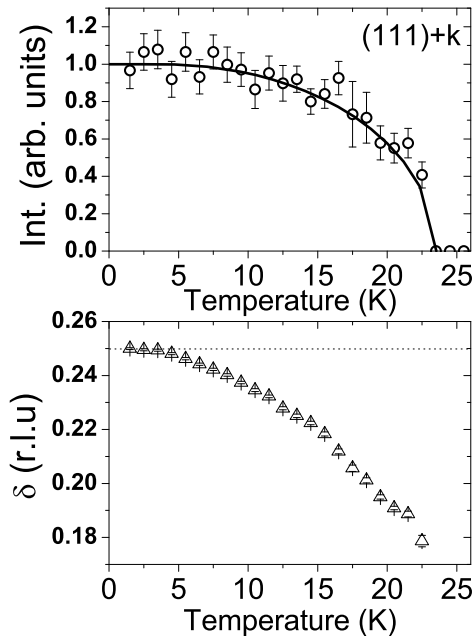


FIG. 3: Upper panel: Integrated intensity of the (111)+k magnetic Bragg peak versus temperature. The solid line is a guide to the eyes. Lower panel: temperature dependence of the propagation vector component δ as a function of temperature. The dotted line indicates the commensurate value $\delta = \frac{1}{4}$

the spontaneous polarization below the magnetic ordering transition, due to the strong reduction of ferromagnetic fluctuations. This is apparently inconsistent with experimental observation, since Weber et al.⁷ report that hysteresis loops become *more pronounced with decreasing temperature*. In light of this temperature variation, it would be particularly interesting to study a direct signature of short-range ferromagnetic order with small angle neutron scattering to explain why ferroelectric order persists below T_N . Additionally, a detailed temperature dependence of the spontaneous polarization is needed to explore the exact nature of ferroelectric ordering.

In summary, we find that non-collinear magnetic ordering develops at 22.5K in HgCr_2S_4 with a spiral structure. Analysis with corepresentation theory shows that magnetic symmetry breaking is inconsistent with the development of a macroscopic polar vector, suggesting another mechanism—such as coupling to short-range ferromagnetic order—as the link between magnetic and electric properties in this material.

Research carried out in the Materials Science Division at Argonne National Laboratory is funded by the US Department of Energy Office of Science, Basic Energy Sciences, under Contract W-31-109-ENG-38.

-
- ¹ M. Kenzelmann, A. B. Harris, S. Jonas, C. Broholm, J. Schefer, S. B. Kim, C. L. Zhang, S.-W. Cheong, O. P. Vajk, and J. W. Lynn, *Phys. Rev. Lett.* **95**, 087206 (2005).
- ² L. C. Chapon, P. G. Radaelli, G. R. Blake, S. Park, and S.-W. Cheong, *Phys. Rev. Lett.* **96**, 097601 (2006).
- ³ L. C. Chapon, G. R. Blake, M. J. Gutmann, S. Park, N. Hur, P. G. Radaelli, and S.-W. Cheong, *Phys. Rev. Lett.* **93**, 177402 (2004).
- ⁴ G. Lawes, M. Kenzelmann, N. Rogado, K. H. Kim, G. A. Jorge, R. J. Cava, A. Aharony, O. Entin-Wohlman, A. B. Harris, T. Yildirim, et al., *Phys. Rev. Lett.* **93**, 247201 (2004).
- ⁵ P. Radaelli and L. Chapon, To be submitted (2006).
- ⁶ J. Hemberger, P. Lunkenheimer, R. Fichtl, H.-A. Krug von Nidda, V. Tsurkan, and A. Loidl, *Nature* **434**, 364 (2005).
- ⁷ S. Weber, P. Lunkenheimer, R. Fichtl, J. Hemberger, V. Tsurkan, and A. Loidl, *Phys. Rev. Lett.* **96**, 157202 (2006).
- ⁸ V. Tsurkan, J. Hemberger, A. Krimmel, H.-A. Krug von Nidda, P. Lunkenheimer, S. Weber, V. Zestrea, and A. Loidl, *Phys. Rev. B* **73**, 224442 (2006).
- ⁹ P. K. Baltzer, P. J. Wojtowicz, M. Robbins, and E. Lopatin, *Phys. Rev.* **151**, 367 (1966).
- ¹⁰ J. M. Hastings and L. M. Corliss, *J. Phys. Chem. Solids* **29**, 9 (1968).
- ¹¹ H. W. Lehmann and G. Harbeke, *Phys. Rev. B* **1**, 319 (1970).
- ¹² O. V. Kovalev, *Representations of the Crystallographic Space Groups, 2^d Edition* (Gordon and Breach Science Publishers, 1993).
- ¹³ J. Rodriguez-Carvajal, *Physica B* **192**, 55 (1993).
- ¹⁴ W. Sikora, F. Bialas, and L. Pytlík, *Journal of Applied Crystallography* **37**, 1015 (2004).
- ¹⁵ T. Borovskaya, L. Butman, V. Tsirel'son, M. Porai-Koshits, T. Aminov, and R. Ozerov, *Kristallografiya* **36**, 612 (1991).
- ¹⁶ L. L.D. and L. E. M., *Statistical Physics, 3d Edition Part1, Course of Theoretical Physics, Volume 5* (BH, 1976).
- ¹⁷ M. Mostovoy, *Phys. Rev. Lett.* **96**, 067601 (2006).
- ¹⁸ The structure is described in the second setting of the International Tables of Crystallography

Irreps	h_1/Kh_{25}	h_4/Kh_{28}	h_{14}/Kh_{38}	h_{15}/Kh_{39}	h_{26}/Kh_2	h_{27}/Kh_{23}	h_{37}/Kh_{13}	h_{40}/Kh_{16}
Γ_5	$\begin{pmatrix} 1 & 0 \\ 0 & 1 \end{pmatrix}$	$\begin{pmatrix} -1 & 0 \\ 0 & -1 \end{pmatrix}$	$\begin{pmatrix} i\epsilon & 0 \\ 0 & -i\epsilon \end{pmatrix}$	$\begin{pmatrix} -i\epsilon & 0 \\ 0 & i\epsilon \end{pmatrix}$	$\begin{pmatrix} 0 & \epsilon \\ \epsilon & 0 \end{pmatrix}$	$\begin{pmatrix} 0 & -\epsilon \\ -\epsilon & 0 \end{pmatrix}$	$\begin{pmatrix} 0 & -i \\ i & 0 \end{pmatrix}$	$\begin{pmatrix} 0 & i \\ -i & 0 \end{pmatrix}$
	$\begin{pmatrix} 0 & 1 \\ 1 & 0 \end{pmatrix}$	$\begin{pmatrix} 0 & -1 \\ -1 & 0 \end{pmatrix}$	$\begin{pmatrix} 0 & i\epsilon^* \\ -i\epsilon^* & 0 \end{pmatrix}$	$\begin{pmatrix} 0 & -i\epsilon^* \\ i\epsilon^* & 0 \end{pmatrix}$	$\begin{pmatrix} \epsilon^* & 0 \\ 0 & \epsilon^* \end{pmatrix}$	$\begin{pmatrix} -\epsilon^* & 0 \\ 0 & -\epsilon^* \end{pmatrix}$	$\begin{pmatrix} -i\epsilon^* & 0 \\ 0 & i\epsilon^* \end{pmatrix}$	$\begin{pmatrix} i\epsilon^* & 0 \\ 0 & -i\epsilon^* \end{pmatrix}$

TABLE II: Matrix representatives of the irreducible co-representation Γ_5 of the little group G_k (space group $G = Fd\bar{3}m$ and $\mathbf{k}=\mathbf{k}_6=(0 \ 0 \ \delta)$). The labels for symmetry operations and numbering of the irreducible representations follow Kovalev's notation. Matrices for unitary (h) and anti-unitary (Kh) symmetry operations are given on the first and second row, respectively. $\epsilon = e^{-i\frac{\pi}{2}\delta}$